Octanuclearity in Copper(II) Chemistry: Preparation, Characterization, and Magnetochemistry of $[Cu_8(dpk{\cdot}OH)_8(O_2CCH_3)_4](ClO_4)_4{\cdot}9H_2O$ ($dpk{\cdot}H_2O$ = the Hydrated, *gem*-Diol Form of Di-2-pyridyl Ketone)

Vasilis Tangoulis, Catherine P. Raptopoulou, and Aris Terzis*

Institute of Materials Science, NRCPS Demokritos, 153 10 Aghia Paraskevi Attikis, Greece

Sofia Paschalidou and Spyros P. Perlepes*

Department of Chemistry, University of Patras, 265 00 Patras, Greece

Evangelos G. Bakalbassis*

Laboratory of Applied Quantum Chemistry, Department of General and Inorganic Chemistry, Faculty of Chemistry, Aristotle University of Thessaloniki, 540 06 Thessaloniki, Greece

Received September 13, 1996[⊗]

The complexes $[Cu_8(dpk{\cdot}OH)_8(O_2CMe)_4](ClO_4)_4{\cdot}9H_2O$ (**1**) and $[Cu(dpk{\cdot}H_2O)_2](O_2CMe)(ClO_4){\cdot}2H_2O$ (**2**), where $dpk{\cdot}H_2O$ is the hydrated, *gem*-diol form of di-2-pyridyl ketone, have been prepared. Complex **1** crystallizes in triclinic space group $P\bar{1}$ with the following unit cell dimensions at 25 °C: $a = 18.396(1)$ Å, $b = 16.720(1)$ Å, $c = 19.171(1)$ Å, $\alpha = 96.10(1)°$, $\beta = 87.68(1)°$, $\gamma = 99.14(1)°$, $Z = 2$. Crystal structure data for **2** at room temperature are as follows: monoclinic, $P2_1/c$, $a = 13.000(2)$ Å, $b = 8.008(1)$ Å, $c = 27.095(3)$ Å, $\beta = 93.19(1)°$, $Z = 4$. The two centrosymmetrically related cubanes in the tetracation of **1** are doubly-bridged with two *syn, anti* acetate groups bridging two Cu^{II} atoms. The monoanion $dpk{\cdot}OH^-$ functions as a $\eta^1{:}\eta^3{:}\eta^1{:}\mu_3$ ligand. Three Cu^{II} atoms have distorted octahedral coordination geometries with CuO_3N_3 and $CuNO_5$ chromophores, while the fourth Cu^{II} center displays a distorted square pyramidal geometry; a terminal monodentate acetate is ligated to this latter Cu^{II} atom. In the mononuclear $[Cu(dpk{\cdot}H_2O)_2]^{2+}$ cation of **2**, the four pyridyl nitrogens can be viewed as strongly coordinating to the metal (Cu−N = 2.013(4)−2.022(4) Å), while one of the hydroxyl oxygens on each ligand forms a weak bond to Cu^{II} (Cu−O = 2.417(4), 2.352(3) Å). Variable-temperature magnetic susceptibility studies on **1** are in line with both an overall antiferromagnetic interaction between Cu^{II} atoms and the magnetic behavior of a simple cubane. Exchange parameters, *J*, derived by using a four-*J* magnetic model, are found to be $J_1 = 6$ cm^{-1}, $J_2 = -144$ cm^{-1}, $J_3 = -14$ cm^{-1}, $J_4 = 3$ cm^{-1} and $g = 2.29$ (adjustable parameter) by least-squares fitting to the spin Hamiltonian $H = -2\sum_{i<j}J_{ij}S_i{\cdot}S_j$. The thus derived energy level spectrum shows a $S = 1$ ground state, further supported by the solid-state and solution EPR spectra of **1**. Insight concerning the effect of structural parameters on the magnitude of the magnetic exchange interactions was gained through EHMO calculations performed on a model $Cu(OR)_2Cu$ moiety. Accordingly, estimates of the *J* parameters, experimentally derived, were in close agreement both with known magneto−structural correlations established for planar $Cu(OR)_2Cu$ moieties and a criterion established by us, holding for the magneto−structural correlations in symmetrical roof-shaped, alkoxo-bridged $Cu(OR)_2Cu$ moieties.

Introduction

Fascination with polynuclear coordination complexes has existed for at least 150 years.[1] Polynuclear metal chemistry is today an area of modern science whose interfaces with many disciplines have provided invaluable opportunities for crossing boundaries both inside and between the fields of chemistry,[2] physics,[3] and biology.[4] This chemistry is of continuing interest for the synthetic inorganic chemists trying to escape from reliance on "spontaneous self-assembly",[5] for scientists seeking to design new molecular materials exhibiting unusual magnetic, optical, and electrical properties,[6] and for bioinorganic chemists investigating the structure and function of polymetallic active sites in metallobiomolecules.[4,7]

[⊗] Abstract published in *Advance ACS Abstracts,* August 1, 1997.

(1) Fremy, E. *Ann. Chim. Phys.* **1852**, *35*, 257.
(2) (a) Dimitrou, K.; Sun, J.-S.; Folting, K.; Christou, G. *Inorg. Chem.* **1995**, *34*, 4160. (b) Zhang, Y.; Thompson, L. K.; Bridson, J. N.; Bubenik, M. *Inorg. Chem.* **1995**, *34*, 5870. (c) Liu, C. W.; Stubbs, T.; Staples, R. J.; Fackler, J. P., Jr. *J. Am. Chem. Soc.* **1995**, *117*, 9778. (d) Chen, X.-M.; Aubin, S. M. J.; Wu, Y.-L.; Yang, Y.-S.; Mak, T. C. W.; Hendrickson, D. N. *J. Am. Chem. Soc.* **1995**, *117*, 9600.
(3) (a) Georges, R.; Kahn, O.; Guillou, O. *Phys. Rev. B* **1994**, *49*, 3235. (b) Taft, K. L.; Papaefthymiou, G. C.; Lippard, S. J. *Science* **1993**, *259*, 1302.
(4) Lippard, S. J.; Berg, J. M. *Principles of Bioinorganic Chemistry*; University Science Books: Mill Valley, CA, 1994.
(5) Libby, E.; Folting, K.; Huffman, C. J.; Huffman, J. C.; Christou, G. *Inorg. Chem.* **1993**, *32*, 2549.
(6) (a) Powell, A. K.; Heath, S. L.; Gatteschi, D.; Pardi, L.; Sessoli, R.; Spina, G.; Giallo, F. D.; Pieralli, F. *J. Am. Chem. Soc.* **1995**, *117*, 2491. (b) Miller, J. S.; Epstein, A. J. *Angew. Chem., Int. Ed. Engl.* **1994**, *33*, 385. (c) *Magnetic Molecular Materials*; Gatteschi, D., Kahn, O., Miller, J. S., Palacio, F., Eds.; NATO ASI Series E, Vol. 198; Kluwer Academic Publishers: Dordrecht, The Netherlands, 1991.
(7) For reviews see : (a) Wieghardt, K. *Angew. Chem., Int. Ed. Engl.* **1989**, *28*, 1153. (b) *Metal Clusters in Proteins*; Que, L., Ed.; ACS Symposium Series *372*; American Chemical Society: Washington, DC, 1988.

S0020-1669(96)01137-8 CCC: $14.00 © 1997 American Chemical Society

The exchange interactions between paramagnetic centers have been intensively investigated in the last 25 years.[8] We can conclude that much is now understood of the details of the interactions in pairs, where the role of both the ground[9] and the excited[10] magnetic orbitals has been clarified, providing a set of rules which extends the original Goodenough−Kanamori rules[11] and allowing the rationalization of the magnetic properties for virtually any magnetic center in any geometry. The type and the magnitude of the magnetic exchange interactions in dinuclear complexes depend on the bridge identity, the M···M separation, the bond angles subtended at the bridging atoms, the dihedral angle between the planes containing the metal ions, the metal−bridge ligand bond lengths, and the metal ion stereochemistries.[12,13] At the other limit, a good understanding has been obtained also for the magnetic interactions in infinite lattices,[8b,9,14] either one-, two-, or three-dimensional, for which both the thermodynamic and dynamic properties have been successfully rationalized and the relations between structural and magnetic dimensionality have been discussed and analyzed. When we look at the field of polynuclear complexes which fall in between these two limits, we see that many details of their magnetic properties have not yet been analyzed. For instance, we can generally explain the magnetic susceptibility of these systems, but we do not have any detailed knowledge of the different total spin states which are thermally populated. In particular, tetranuclear complexes have up to now resisted all attempts to obtain a deep knowledge of the low-lying energy levels,[15] although they include systems of great interest, such as the 4Fe−4S proteins and the Mn_4 aggregate in the photosynthetic water oxidation center (WOC).[4] Even in the relatively simple case of four copper(II) ions, where four $S = {}^1/_2$ states are coupled to give a quintet, three triplet, and two singlet electronic levels, many difficulties exist and much controversy is present in the literature concerning the relative order of the various multiplets.[15,16]

Chart 1

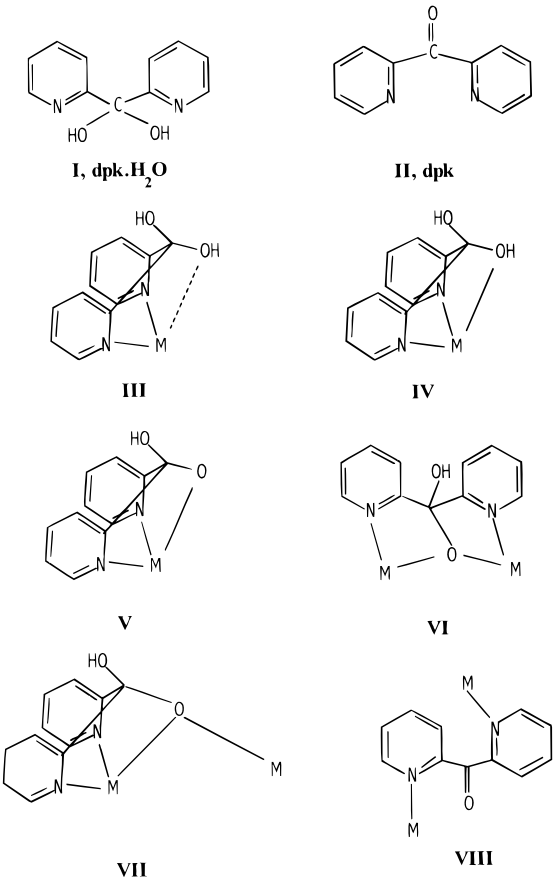

The presence of both bulky ligands that diminish exchange interactions between clusters in the crystal lattice and sufficiently large intracluster exchange interaction to result in clear splittings of the ground-state levels allows for an adequate characterization of the low-lying levels present in these systems.[15] In searching for tetranuclear copper(II) clusters which fulfill these two necessary requirements, we report here the preparation, crystal structure, and magnetic properties of the remarkable *octanuclear* complex $[Cu_8(dpk{\cdot}OH)_8(O_2CMe)_4](ClO_4)_4{\cdot}9H_2O$ (**1**) featuring an acetato-bridged dicubane core, where dpk·OH^- is the monoanion of the hydrated *gem*-diol form of di-2-pyridyl ketone (dihydroxy-di-2-pyridylmethane, **I**; Chart 1). Although polynuclear copper(II) complexes containing up to six metal atoms are not rare, compounds with seven,[17] eight[18] or more[19] copper-

(8) Some recent papers: (a) Goldberg, D. P.; Telser, J.; Bastos, C. M.; Lippard, S. J. *Inorg.Chem.* **1995**, *34*, 3011. (b) De Munno, G.; Julve, M.; Lloret, F.; Cano, J.; Caneschi, A. *Inorg. Chem.* **1995**, *34*, 2048. (c) Castro, I.; Sletten, J.; Calatayud, M.; Julve, M.; Cano, J.; Lloret, F.; Caneschi, A. *Inorg. Chem.* **1995**, *34*, 4903. (d) Bürger, K.-S.; Chaudhuri, P.; Wieghardt, K.; Nuber, B. *Chem. Eur. J.* **1995**, *1*, 583. (e) Bakalbassis, E. G.; Diamantopoulou, E.; Perlepes, S. P.; Raptopoulou, C. P.; Tangoulis, V.; Terzis, A.; Zafiropoulos, Th. F. *J. Chem. Soc., Chem. Commun.* **1995**, 1347.

(9) *Magneto-Structural Correlations in Exchange Coupled Systems*; Willet, R. D., Gatteschi, D., Kahn, O., Eds.; D. Reidel: Dordrecht, The Netherlands, 1985.

(10) (a) Banci, L.; Bencini, A.; Gatteschi, D. *J. Am. Chem. Soc.* **1983**, *105*, 761. (b) Bencini, A.; Gatteschi, D.; Zanchini, C. *Inorg. Chem.* **1985**, *24*, 704. (c) Charlot, M. F.; Journaux, Y.; Kahn, O.; Bencini, A.; Gatteschi, D.; Zanchini, C. *Inorg. Chem.* **1986**, *25*, 1060.

(11) (a) Goodenough, J. B. In *Magnetism and the Chemical Bond*; Interscience: New York, 1963. (b) Kanamori, J. In *Magnetism*; Rado, G. T., Suhl, H., Eds.; Academic Press: New York, 1963; Vol. 1; p 161. (c) Kanamori, J. *J. Phys. Chem. Solids* **1959**, *10*, 87.

(12) For reviews see: (a) Kato, M.; Muto, Y. *Coord. Chem. Rev.* **1988**, *92*, 45. (b) Kahn, O. *Angew. Chem., Int. Ed. Engl.* **1985**, *24*, 834. (c) Kahn, O. *Comments Inorg. Chem.* **1984**, *3*, 105. (d) Melnik, M. *Coord. Chem. Rev.* **1982**, *42*, 259. (e) Doedens, R. J. *Prog. Inorg. Chem.* **1976**, *21*, 209. (f) Hodgson, D. J. *Prog. Inorg. Chem.* **1975**, *19*, 173.

(13) Tandon, S. S.; Thompson, L. K.; Manuel, M. E.; Bridson, J. N. *Inorg. Chem.* **1994**, *33*, 5555.

(14) (a) Papadopoulos, A. N.; Tangoulis, V.; Raptopoulou, C. P.; Terzis, A.; Kessissoglou, D. P. *Inorg. Chem.* **1996,** *35*, 559. (b) De Munno, G.; Julve, M.; Lloret, F.; Faus, J.; Verdaguer, M.; Caneschi, A. *Inorg. Chem.* **1995**, *34*, 157. (c) Borras-Almenar, J. J.; Coronado, E.; Curely, J.; Georges, R. *Inorg. Chem.* **1995**, *34*, 2699. (d) Chiari, B.; Cinti, A.; Piovesana, O.; Zanazzi, P. F. *Inorg. Chem.* **1995**, *34*, 2652. (e) Borras-Almenar, J. J.; Coronado, E.; Curely, J.; Georges, R.; Gianduzzo, J. C. *Inorg. Chem.* **1994**, *33*, 5171. (f) Ribas, J.; Monfort, M.; Solans, X.; Drillon, M. *Inorg. Chem.* **1994**, *33*, 742. (g) *Extended Linear Chain Systems*; Miller, J. S., Ed.; Plenum Press: New York, 1982.

(15) Bencini, A.; Gatteschi, D.; Zanchini, C.; Haasnoot, J. G.; Prins, R.; Reedijk, J. *J. Am. Chem. Soc.* **1987**, *109*, 2926.

(16) (a) Buluggiu, E. *J. Chem. Phys.* **1986**, *84*, 1243. (b) Black, T. D.; Rubins, R.; De, D. K.; Dickinson, R. C.; Baker, W. A., Jr. *J. Chem. Phys.* **1984**, *80*, 4620.

(17) (a) Blake, A. J.; Gould, R. O.; Grant, C. M.; Milne, P. E. Y.; Reed, D.; Winpenny, R. E. P. *Angew. Chem., Int. Ed. Engl.* **1994**, *33*, 195. (b) Real, J. A.; De Munno, G.; Chiappetta, R.; Julve, M.; Lloret, F.; Journaux, Y.; Colin, J.-C.; Blondin, G. *Angew. Chem., Int. Ed. Engl.* **1994**, *33*, 1184.

(18) (a) Blake, A. J.; Grant, C. M.; Gregory, C. I.; Parsons, S.; Rawson, J. M.; Reed, D.; Winpenny, R. E. P. *J. Chem. Soc., Dalton Trans.* **1995**, 163. (b) Zhang, Y.; Thompson, L. K.; Bridson, J. N.; Bubenik, M. *Inorg. Chem.* **1995**, *34*, 5870. (c) Ardizzoia, G. A.; Angaroni, M. A.; La Monica, G.; Cariati, F.; Cenini, S.; Moret, M.; Masciocchi, N. *Inorg. Chem.* **1991**, *30*, 4347. (d) McKee, V.; Tandon, S. S. *J. Chem. Soc., Dalton Trans.* **1991**, 221. (e) Agostinelli; Dell'Amoco, D. B.; Calderazzo, F.; Fiorani, D.; Pelizzi, G. *Gazz. Chim. Ital.* **1988**, *118*, 729. (f) Galy, J.; Mosset, A.; Grenthe, I.; Puigdomènech, I.; Sjøberg, B.; Hulten, F. *J. Am. Chem. Soc.* **1987**, *109*, 380.

(19) (a) Tandon, S. S.; Thompson, L. K.; Bridson, J. N.; Benelli, C. *Inorg. Chem.* **1995**, *34*, 5507. (b) Norman, R. E.; Rose, N. J.; Stenkamp, R. E. *J. Chem. Soc., Dalton Trans.* **1987**, 2905. (c) Turpeinen, U.; Hämäläinen; Reedijk, J. *Inorg. Chim. Acta* **1987**, 134, 87. (d) Watson, W. H.; Holley, W. W. *Croat. Chem. Acta* **1984**, *57*, 467.

(II) atoms remain rare. A more general objective in our laboratories is to investigate the ability of ligands derived from di-2-pyridyl ketone (**II**; hereafter abbreviated as dpk) to stabilize polynuclear metal carboxylate assemblies. Literature data[20] indicate that dpk forms complexes with a range of metal ions and easily undergoes hydration on complex formation to give complexes containing dpk·H_2O or dpk·OH^-, whereas hydration of ketone does not occur to any significant extent in aqueous solution in the absence of the metal ion.[20c] Several reasons for the hydration behavior have been presented.[20e,f] The dpk·H_2O, dpk·OH^-, and dpk ligands have been shown to be capable of binding to transition metals in a rather limited number of different ways. Single-crystal X-ray analyses of a few complexes have established binding modes **III**−**VIII** to be those observed.[20] Also described in this paper are the preparation and characterization of the monomeric complex [Cu(dpk·$H_2O)_2$](O_2CMe)(ClO_4)·$2H_2O$ (**2**), which is synthetically relevant to complex **1**. Portions of this work have been recently communicated.[22] The experimental results for **1**, along with the results of an EHMO calculation performed on the model $Cu(OR)_2Cu$ moiety, enables us to both (i) elucidate the experimentally derived estimates of the *J* parameters and (ii) establish a new criterion, holding for the magneto−structural correlations in symmetrical roof-shaped, alkoxo-bridged $Cu(OR)_2Cu$ moieties.

Experimental Section

Materials. All manipulations were performed under aerobic conditions using materials as received (Aldich Co.); water was distilled in-house. All chemicals and solvents were of reagent grade.

Physical Measurements. Elemental analyses for carbon, hydrogen, and nitrogen were performed at the Microanalytical Laboratory, Department of Chemistry, University of Dortmund, Dortmund, Germany. Copper analysis was carried out by EDTA titration. Conductivity measurements were carried out with a Metrohm-Herisau E-527 bridge and a cell of standard constant. Infrared spectra (4000−450 cm^{-1}) were recorded on a Perkin-Elmer 16 PC infrared spectrometer with samples prepared as KBr pellets. Solid-state (diffuse reflectance, 890−340 nm) and solution (800−300 nm) electronic spectra were recorded on Varian 634 and Biochrom 4060 instruments, respectively. Solution- and solid-state EPR spectra were recorded in the 295−4.5 K temperature range, on a Bruker ER 200D-SRC X-band spectrometer equipped with an Oxford ESR 9 cryostat. Room-temperature magnetic measurements were carried out by Faraday's method using a Cahn-Ventron RM-2 balance standardized with $HgCo(NCS)_4$. Variable-temperature magnetic susceptibility measurements were carried out on a polycrystalline sample of **1** in the 300−5.0 K temperature range using a Quantum Design Squid susceptometer by applying magnetic fields of 1000 and 6000 G. The correction for the diamagnetism of the complex was estimated from the Pascal constants; a value of 60×10^{-6} cm^3 mol^{-1} was used for the TIP of the Cu(II) ion. The magnetism of the sample was found to be field independent. For all the magnetic studies we used a molecular weight without the nine solvent water molecules, based on our experience with the X-ray data collection (*vide infra*). However, chemical analysis of two portions from the powder sample used for the magnetic measurements indicated that some water molecules were retained. This introduces a systematic error in the susceptibility data.[21]

Initial Preparations of Compounds 1 and 2 in a Mixture. [$Cu_2(O_2CMe)_4(H_2O)_2$] (0.24 g, 0.6 mmol) and dpk (0.26 g, 1.4 mmol) were dissolved in warm H_2O (20 mL). The resulting blue-violet solution was stirred while an aqueous solution (10 mL) of $NaClO_4$·H_2O (0.17 g, 1.2 mmol) was added to give a homogeneous solution of the same color. This was allowed to slowly concentrate by evaporation at room temperature to give a mixture of green and violet crystals. These were carefully collected by filtration. The two products were readily separable manually, and the green and violet prismatic crystals proved by single-crystal X-ray crystallography to be complexes [Cu_8(dpk·OH)$_8$(O_2CMe)$_4$](ClO_4)$_4$·$9H_2O$ (**1**) and [Cu(dpk·$H_2O)_2$](O_2CMe)(ClO_4)·$2H_2O$ (**2**), respectively.

[Cu_8(dpk·OH)$_8$(O_2CMe)$_4$](ClO_4)$_4$·$9H_2O$ (1). Method A. A stirred blue-green solution of [$Cu_2(O_2CMe)_4(H_2O)_2$] (0.24 g, 0.6 mmol) in H_2O (11 mL) was added to a solution of dpk (0.22 g, 1.2 mmol) in H_2O (9 mL). To the resultant blue solution an aqueous solution (10 mL) of $NaClO_4$·H_2O (0.084 g, 0.6 mmol) was added; no noticeable color change occurred. The solution was exposed to air and left for slow evaporation. A green crystalline material was deposited in a couple of days, which was collected by filtration, washed with cold EtOH and Et_2O, and dried in air. The yield was ∼30% based on Cu. Anal. Calcd (found) for $C_{96}H_{102}N_{16}O_{49}Cl_4Cu_8$: C, 39.56 (40.01); H, 3.53 (3.41); N, 7.69 (7.77); Cu, 17.44 (16.90). These analytical data refer to crystals of the complex. IR data (KBr pellet, cm^{-1}): 3385 (s, br), ∼3300 (m, br), 2915 (w), 2880 (sh), 1602 (s), 1590 (sh), 1472 (m), 1446 (s), 1338 (m), 1300 (sh), 1296 (w), 1260 (w), 1222 (m), 1122 (s), 1076 (vs), 1048 (s), 1014 (m), 970 (vw), 956 (m), 902 (w), 804 (m), 782 (m), 766 (m), 740 (vw), 686 (m), 654 (w), 636 (m), 624 (s), 598 (w), 560 (w), 498 (w), 460 (w). Solid-state (diffuse reflectance) electronic spectrum (λ_{max}, nm): 370, 725. Electronic spectrum [λ_{max}, nm (ϵ_M/Cu_8, L mol^{-1} cm^{-1})] in $MeNO_2$: 374 (1400), 733 (360). Molar conductivity for a $\sim 10^{-3}$ M solution in $MeNO_2$: 322 S cm^2 mol^{-1}.

Method B. A stirred solution of $CuCl_2$·$2H_2O$ (0.28 g, 1.6 mmol) in H_2O (13 mL) was treated with solid NaO_2CMe·$3H_2O$ (0.11 g, 0.8 mmol) and $NaClO_4$·H_2O (0.11 g, 0.8 mmol). The resulting blue-green solution was stirred while an aqueous solution (20 mL) containing NaOH (0.064 g, 1.6 mmol) and dpk (0.30 g, 1.6 mmol) was added to produce a green solution. The latter was concentrated in vacuo at 55 °C to yield a green microcrystalline solid. This was washed with cold EtOH and Et_2O (not added in the filtrate) and dried in air. The yield was ∼35% based on Cu. Additional solid (∼15% yield) can be obtained from the filtrate on further concentration for 1−2 weeks, for a combined yield of ∼50%. The identity of the product was confirmed by IR and UV/vis spectroscopic comparison with samples from method A.

[Cu(dpk·$H_2O)_2$](O_2CMe)(ClO_4)·$2H_2O$ (2). Solid [$Cu_2(O_2CMe)_4$($H_2O)_2$] (0.24 g, 0.6 mmol) was dissolved with stirring in a solution of dpk (0.44 g, 2.4 mmol) in H_2O (23 mL). A deep blue-violet homogeneous solution was obtained, and to this was added a solution of $NaClO_4$·H_2O (0.17 g, 1.2 mmol) in H_2O (7 mL). The solution was allowed to stand undisturbed at room temperature overnight. Well-formed, X-ray-quality crystals of **2** slowly appeared. The violet crystals were collected by filtration, washed with a little cold H_2O, and dried *in vacuo* over P_4O_{10}. The yield was ∼60%. Anal. Calcd (found) for $C_{24}H_{27}N_4O_{12}ClCu$: C, 43.51 (44.00); H, 4.12 (4.05); N, 8.46 (8.40); Cu, 9.59 (10.12). IR data (KBr pellet, cm^{-1}): 3554 (m), 3420 (m, br), ∼3200 (m, br), 3122 (m), 3018 (m), 2920 (w), 2870 (w), 1606 (m), 1570 (sh), 1558 (m), 1470 (m), 1446 (s), 1425 (sh), 1342 (w), 1312 (w), 1302 (w), 1270 (w), 1228 (s), 1176 (s), 1158 (s), 1122 (vs), 1094 (vs), 1030 (s), 978 (w), 930 (w), 900 (w), 838 (w, br), 804 (s), 764 (s), 672 (m), 656 (m), 624 (s), 576 (w), 508 (w), 496 (w), 492 (w), 480 (w). Electronic spectrum [λ_{max}, nm (ϵ_M, L mol^{-1} cm^{-1})] in MeOH: 330 (770), 595 (75). Solid-state effective magnetic moment: $\mu_{eff} = 1.94\ \mu_B$ (∼25 °C).

Caution! *Perchlorate salts are potentially explosive. Although no detonation tendencies have been observed with **1** and **2**, caution is advised and handling of only small quantities is recommended.*

X-ray Crystallography. A green prismatic crystal of **1** with approximate dimensions $0.34 \times 0.22 \times 0.50$ mm and a violet prismatic

(20) (a) Sommerer, S. O.; Westcott, B. L.; Abboud, K. A. *Acta Crystallogr., Sect. C* **1994**, *50*, 48. (b) Sommerer, S. O.; Abboud, K. A. *Acta Crystallogr. Sect. C* **1993**, *49*, 1152. (c) Sommerer, S.; Jensen, W. P.; Jacobson, R. A. *Inorg. Chim. Acta* **1990**, *172*, 3. (d) Wang, S.-L.; Richardson, J. W., Jr.; Briggs, S. J.; Jacobson, R. A.; Jensen, W. P. *Inorg. Chim. Acta* **1986**, *111*, 67. (e) Byers, P. K.; Canty, A. J.; Engelhardt, L. M.; Patrick, J. M.; White, A. H. *J. Chem. Soc., Dalton Trans*. **1985**, 981. (f) Annibale, G.; Canovese, L.; Cattalini, L.; Natile, G.; Biagini-Cingi, M.; Manotti-Lanfredi, A.-M.; Tiripicchio, A. *J. Chem. Soc., Dalton Trans*. **1981**, 2280. (g) Breeze, S. R.; Wang, S.; Greedan, J. E.; Raju, N. P. *Inorg. Chem.* **1996**, *35*, 6944.

(21) Kolks, G.; Lippard, S. J.; Waszczak, J. V.; Lilienthal, H. R. *J. Am. Chem. Soc.* **1982**, *104*, 717.

(22) Tangoulis, V.; Paschalidou, S.; Bakalbassis, E.; Perlepes, S. P.; Raptopoulou, C. P.; Terzis, A. *Chem. Commun*. **1996**, 1297.

Table 1. Crystallographic Data for Complex **2**

param	**2**
formula	$C_{24}H_{27}N_4O_{12}ClCu$
fw	662.49
space group	$P2_1/c$
temp, °C	25
λ, Å	0.71073
a, Å	13.000(2)
b, Å	8.008(1)
c, Å	27.095(3)
α, deg	
β, deg	93.19(1)
γ, deg	
V, Å^3	2816.4(6)
Z	4
ρ_{calc}, g cm^{-3}	1.562
μ(Mo Kα), mm^{-1}	0.940
$R1$[a]	0.0629
$wR2$[a]	0.1721

[a] $w = 1/[\sigma^2(F_o^2) + (aP)^2 + bP]$ and $P_2 = (\max(F_o^2,0) + 2F_c^2)/3$; $a = 0.1033$, $b = 6.3329$. $R1 = \sum(||F_o| - |F_c||)/\sum(|F_o|)$, $wR2 = \{\sum[w(F_o^2 - F_c^2)^2]/\sum[w(F_o^2)^2]\}^{1/2}$ for reflections with $I > 2\sigma(I)$.

crystal of **2** with approximate dimensions 0.20 × 0.30 × 0.50 mm were mounted in capillary filled with drops of mother liquid and in air, respectively. An attempt to collect data for **1** in air failed due to crystal deterioration. Diffraction measurements were made on a Crystal Logic Dual Goniometer diffractometer using graphite-monochromated Mo radiation. Complete crystal data and parameters for data collection for complex **2** are reported in Table 1. Unit cell dimensions were determined and refined by using the angular settings of 25 automatically centered reflections in the range $11° < 2\theta < 23°$. Intensity data were recorded using a $\theta-2\theta$ scan to $2\theta(\max) = 50°$ with scan speed 4.5 deg/min for **1** and 4.2 deg/min for **2**, and scan range 2.4 plus $\alpha_1\alpha_2$ separation. Three standard reflections, monitored every 97 reflections showed less than 3% intensity fluctuation and no decay. Lorentz, polarization, and ψ-scan absorption corrections were applied using Crystal Logic software.

Symmetry-equivalent data for **1** and **2** were averaged with $R = 0.0212$ and 0.0175, respectively, to give 20 239 and 4965 independent reflections from a total 20 914 and 5202 collected. The structures were solved by direct methods using SHELXS-86[23a] and refined by full-matrix least-squares techniques on F^2 with SHELXL-93[23b] using 20 237 (**1**) and 4964 (**2**) reflections and refining 1486 and 464 parameters, respectively. For **1**, all hydrogen atoms of the pyridine rings of dpk·OH$^-$ and those of the acetate ions were introduced at calculated positions as riding on bonded atoms and refined isotropically. The oxygen atoms of three perchlorate ions and the water molecules were refined isotropically; the fourth perchlorate ion was found disordered, and the refinement was carried out by considering two positions for the chlorine atom (each having occupation factor fixed at 10.5). Two oxygen atoms were considered common. The other two were disordered and they were refined in two positions with occupation factors fixed at 10.5. All the rest non-hydrogen atoms were refined anisotropically. Almost all hydrogen atoms of **2** (except those of the methyl C(24) group which were introduced at calculated positions as riding on a bonded atom) were located by difference maps and refined isotropically. The perchlorate counterion was found disordered and refined isotropically by considering the oxygen atoms in two different orientations. The remaining non-hydrogen atoms were refined anisotropically. The final values of $R1$ and $wR2$ for **1** are 0.0699 and 0.1763 for all data and 0.0550 and 0.1607 for 16 163 reflections with $I > 2\sigma(I)$; for **2** they are 0.0816 and 0.1911 for all data and for observed data are listed in Table 1. The maximum and minimum residual peaks in the final difference map were 1.304 and −0.997 e Å^{-3} for **1** and 1.007 and −1.334 e Å^{-3} for **2**. The largest shift/esd in the final cycle was 0.941 for **1** and 0.145 for **2**.

(23) (a) Sheldrick, G. M. SHELXS-86, Structure Solving Program. University of Göttingen, Germany, 1986. (b) Sheldrick, G. M., SHELXL-93, Crystal Structure Refinement, University of Göttingen, Germany, 1993.

Results and Discussion

Synthesis. The present work represents one of the first stages[8e] of a program concerned with developing synthetic methodologies to high-nuclearity M_x (M = Mn, Fe, Co, Ni, Cu; $x \geq 4$) aggregates. One of our strategies takes advantage of the observation that the reactions between metal carboxylates and dpk in H_2O or H_2O-containing organic solvents are excellent springboards to a variety of such products. Obviously dpk·H_2O can be fully or partially deprotonated by the RCO_2^- groups of the metal carboxylate, and we reasoned that new types of polynuclear M/RCO_2^-/dpk·OH^- or dpk·O^{2-} species might result (as long as the RCO_2^-:dpk ratio was high enough to leave an amount of nonprotonated RCO_2^- ions in the reaction mixture) given the fact that both RCO_2^- and dpk·OH^-/dpk·O^{2-} can potentially adopt bridging and terminal modes. This has, indeed, turned out to be case.

Treatment of $[Cu_2(O_2CMe)_4(H_2O)_2]$ with 2.3−2.4 equiv of dpk in H_2O followed by addition of $NaClO_4$·H_2O yielded color changes and, finally, a blue-violet solution that slowly deposited a mixture of well-formed green and violet crystals; these crystals proved to be complexes **1** and **2**, respectively, by single-crystal X-ray crystallography. With the identities of **1** and **2** established, preparative routes to pure materials were subsequently devised by modifying the $[Cu_2(O_2CMe)_4(H_2O)_2]$:dpk:ClO_4^- molar ratio (eqs 1 and 2).

$$4[Cu_2(O_2CMe)_4(H_2O)_2] + 8dpk + 8H_2O + 4NaClO_4\cdot H_2O \xrightarrow{H_2O} \underset{\mathbf{1}}{[Cu_8(dpk\cdot OH)_8(O_2CMe)_4](ClO_4)_4\cdot 9H_2O} + 8MeCO_2H + 4NaO_2CMe + 3H_2O \quad (1)$$

$$[Cu_2(O_2CMe)_4(H_2O)_2] + 4dpk + 4H_2O + 2NaClO_4\cdot H_2O \xrightarrow{H_2O} \underset{\mathbf{2}}{2[Cu(dpk\cdot H_2O)_2](O_2CMe)(ClO_4)\cdot 2H_2O} + 2NaO_2CMe \quad (2)$$

A second clean route to **1** (method B in the Experimental Section) was also developed by employing $CuCl_2$, NaOH (for the deprotonation of dpk·H_2O), and NaO_2CMe (as the source of the necessary $MeCO_2^-$) as reactants (eq 3). Complex **1** seems to be an 1:4 electrolyte in a $\sim 10^{-3}$ M $MeNO_2$ solution (Λ_M = 322 S cm^2 mol^{-1}).[24]

$$8CuCl_2\cdot 2H_2O + 8dpk + 8H_2O + 8NaOH + 4NaClO_4\cdot H_2O + 4NaO_2CMe\cdot 3H_2O \xrightarrow{H_2O} \underset{\mathbf{1}}{[Cu_8(dpk\cdot OH)_8(O_2CMe)_4](ClO_4)_4\cdot 9H_2O} + 16NaCl + 31H_2O \quad (3)$$

Description of Structures. Selected interatomic distances and angles for **1** and **2** are collected in Tables 2 and 3, respectively. A portion of the cation of complex **1** is provided in Figure 1. The structure of the cation of complex **2** is shown in Figure 2.

A partial description of **1** has already been given.[22] The unit cell of **1** contains two $[Cu_8(dpk\cdot OH)_8(O_2CMe)_4]^{4+}$ cations, each lying on an inversion center and each comprising a distorted, double cubane. Each cube is completed by four deprotonated oxygen atoms from the dpk·OH^- ligands at alternating vertices.

(24) Geary, W. J. *Coord. Chem. Rev.* **1971**, *7*, 81.

Table 2. Selected Interatomic Distances (Å) and Angles (deg) for Complex **1**[a]

Distances							
Cu(1)···Cu(2)	3.304(1)	Cu(1)···Cu(4)	3.004(1)	Cu(2)···Cu(4)	3.527(1)	Cu(3)···Cu(3′)	4.913(1)
Cu(1)···Cu(3)	3.472(1)	Cu(2)···Cu(3)	3.038(1)	Cu(3)···Cu(4)	3.377(1)		
Cu(1)−N(1)	1.997(4)	Cu(2)−N(12)	2.011(4)	Cu(3)−N(32)	2.003(4)	Cu(4)−N(2)	2.210(4)
Cu(1)−N(11)	2.102(4)	Cu(2)−O(1)	2.357(3)	Cu(3)−O(11)	1.971(3)	Cu(4)−N(22)	2.008(4)
Cu(1)−N(21)	2.187(4)	Cu(2)−O(11)	1.937(3)	Cu(3)−O(21)	2.480(3)	Cu(4)−N(31)	2.050(4)
Cu(1)−O(1)	2.058(3)	Cu(2)−O(31)	1.996(3)	Cu(3)−O(31)	1.932(3)	Cu(4)−O(1)	1.982(3)
Cu(1)−O(11)	2.565(3)	Cu(2)−O(113)	1.913(4)	Cu(3)−O(111)	1.933(4)	Cu(4)−O(21)	2.033(3)
Cu(1)−O(21)	1.977(3)			Cu(3)−O(112′)	2.711(4)	Cu(4)−O(31)	2.632(3)

Angles							
N(1)−Cu(1)−N(11)	98.5(2)	N(12)−Cu(2)−O(1)	105.8(1)	N(32)−Cu(3)−O(11)	160.1(2)	N(2)−Cu(4)−N(22)	98.5(2)
N(1)−Cu(1)−N(21)	101.2(2)	N(12)−Cu(2)−O(11)	81.2(2)	N(32)−Cu(3)−O(21)	95.5(1)	N(2)−Cu(4)−N(31)	103.9(2)
N(1)−Cu(1)−O(1)	80.5(2)	N(12)−Cu(2)−O(31)	157.8(2)	N(32)−Cu(3)−O(31)	81.8(2)	N(2)−Cu(4)−O(1)	77.3(1)
N(1)−Cu(1)−O(11)	106.0(1)	N(12)−Cu(2)−O(113)	99.1(2)	N(32)−Cu(3)−O(111)	96.0(2)	N(2)−Cu(4)−O(21)	107.0(1)
N(1)−Cu(1)−O(21)	159.9(2)	O(1)−Cu(2)−O(11)	86.7(1)	N(32)−Cu(3)−O(112′)	84.4(1)	N(2)−Cu(4)−O(31)	148.5(2)
N(11)−Cu(1)−N(21)	101.2(2)	O(1)−Cu(2)−O(31)	79.8(1)	O(11)−Cu(3)−O(21)	80.7(1)	N(22)−Cu(4)−N(31)	99.7(2)
N(11)−Cu(1)−O(1)	147.6(1)	O(1)−Cu(2)−O(113)	87.6(1)	O(11)−Cu(3)−O(31)	78.5(1)	N(22)−Cu(4)−O(1)	160.1(2)
N(11)−Cu(1)−O(11)	70.2(1)	O(11)−Cu(2)−O(31)	77.7(1)	O(11)−Cu(3)−O(111)	103.1(1)	N(22)−Cu(4)−O(21)	81.1(2)
N(11)−Cu(1)−O(21)	101.4(2)	O(11)−Cu(2)−O(113)	174.1(2)	O(11)−Cu(3)−O(112′)	96.3(1)	N(22)−Cu(4)−O(31)	113.0(1)
N(21)−Cu(1)−O(1)	110.8(2)	O(31)−Cu(2)−O(113)	102.6(2)	O(21)−Cu(3)−O(31)	85.9(1)	N(31)−Cu(4)−O(1)	100.1(2)
N(21)−Cu(1)−O(11)	152.4(2)	Cu(1)−O(11)−Cu(3)	99.1(1)	O(21)−Cu(3)−O(111)	85.2(1)	N(31)−Cu(4)−O(21)	148.7(1)
N(21)−Cu(1)−O(21)	77.8(2)	Cu(1)−O(21)−Cu(3)	101.7(1)	O(21)−Cu(3)−O(112′)	170.9(2)	N(31)−Cu(4)−O(31)	70.8(1)
O(1)−Cu(1)−O(11)	78.9(1)	Cu(1)−O(21)−Cu(4)	97.0(1)	O(31)−Cu(3)−O(111)	170.5(2)	O(1)−Cu(4)−O(21)	81.6(1)
O(1)−Cu(1)−O(21)	81.1(1)	Cu(2)−O(1)−Cu(4)	108.5(1)	O(31)−Cu(3)−O(112′)	85.1(1)	O(1)−Cu(4)−O(31)	73.4(1)
O(11)−Cu(1)−O(21)	78.4(1)	Cu(2)−O(11)−Cu(3)	102.0(1)	O(111)−Cu(3)−O(112′)	103.9(1)	O(21)−Cu(4)−O(31)	80.0(1)
Cu(1)−O(1)−Cu(2)	96.7(1)	Cu(2)−O(31)−Cu(3)	101.3(1)	Cu(3)−O(21)−Cu(4)	96.4(1)		
Cu(1)−O(1)−Cu(4)	96.0(1)	Cu(2)−O(31)−Cu(4)	98.4(1)	Cu(3)−O(31)−Cu(4)	94.2(1)		
Cu(1)−O(11)−Cu(2)	93.4(1)						

[a] Only distances and angles for one $[Cu_8(dpk{\cdot}OH)_8(O_2CMe)_4]^{4+}$ cation of the unit cell are listed.

Table 3. Selected Interatomic Distances (Å), Angles (deg), and Hydrogen-Bonding Interactions for Complex **2**

Distances			
Cu−N(1)	2.017(4)	Cu−N(4)	2.013(4)
Cu−O(1)	2.417(4)	C(6)−O(1)	1.423(6)
Cu−N(2)	2.022(4)	C(6)−O(2)	1.377(6)
Cu−N(3)	2.020(4)	C(17)−O(3)	1.421(6)
Cu−O(3)	2.352(3)	C(17)−O(4)	1.376(6)

Angles			
N(1)−Cu−O(1)	75.4(1)	O(1)−Cu−N(4)	100.6(1)
N(1)−Cu−N(2)	87.3(2)	N(2)−Cu−N(3)	178.6(2)
N(1)−Cu−N(3)	93.5(2)	N(2)−Cu−O(3)	101.8(1)
N(1)−Cu−O(3)	109.4(1)	N(2)−Cu−N(4)	91.1(2)
N(1)−Cu−N(4)	176.0(1)	N(3)−Cu−O(3)	76.9(1)
O(1)−Cu−N(2)	74.1(1)	N(3)−Cu−N(4)	88.1(2)
O(1)−Cu−N(3)	107.2(1)	O(3)−Cu−N(4)	74.5(1)
O(1)−Cu−O(3)	173.7(1)	O(1)−C(6)−O(2)	112.9(4)
		O(3)−C(17)−O(4)	113.7(4)

Hydrogen Bonds[a−c]

D	H	A	D···A, Å	D−H···A, deg
O(1)	H(O1)	O(W1)[i]	2.73(1)	
O(1)	H(O1)	O(W1)[i]	2.73(1)	167(5)
O(2)	H(O2)	O(W1)[ii]	2.73(1)	169(1)
O(3)	H(O3)	O(6)	2.59(1)	178(1)
O(4)	HO(4)	O(6)[iii]	2.61(1)	165(5)
O(W1)	H(W1A)	O(10)[iv]	2.87(1)	166(7)
O(W1)	H(W1B)	O(W2)	2.63(1)	169(5)
O(W2)	H(W2A)	O(5)[v]	2.66(1)	177(1)
O(W2)	H(W2B)	O(8')[vi]	2.96(1)	168(1)

[a] Symmetry operations: (i) $x, y-1, z$; (ii) $1-x, 1-y, -z$; (iii) $2-x, -0.5+y, 0.5-z$; (iv) $1-x, 1.5+y, 0.5-z$; (v) $1-x, 0.5+y, 0.5-z$; (vi) $1-x, 0.5+y, 0.5-z$. [b] A = acceptor, D = donor. [c] Atoms O(5) and O(6) belong to the acetate counterion, while O(8′) and O(10) are from the perchlorate group.

The structures of the two independent cubanes are very similar, and only the Cu(1)−Cu(4) one will be further discussed. No direct bonding exists between the two crystallographically independent cubanes.

One oxygen atom of each dpk·OH$^-$ remains protonated and unbound to the metals. The resulting monoanion functions as

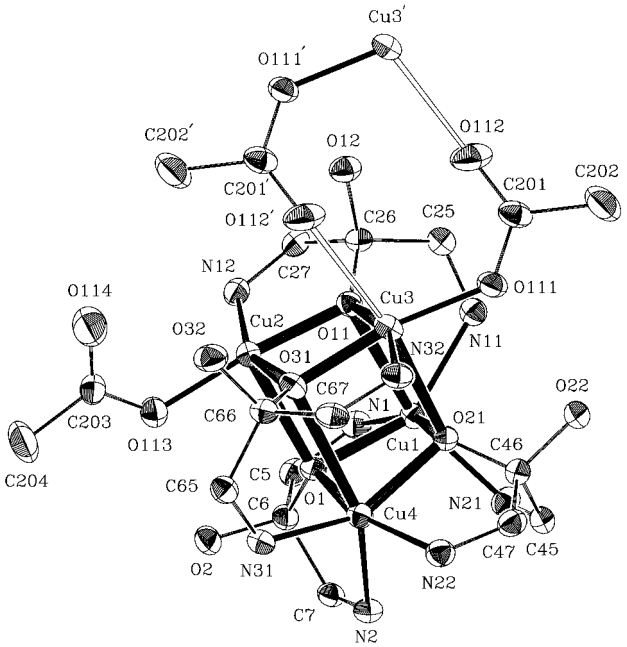

Figure 1. ORTEP representation of a portion of one cation of complex **1** at the 30% probability level. Note that both intercubane bridging acetates are shown. Most aromatic carbon atoms of dpk·OH$^-$ have been omitted for clarity.

a $\eta^1{:}\eta^3{:}\eta^1{:}\mu_3$ ligand (**IX**) forming two five-membered CuNCCO

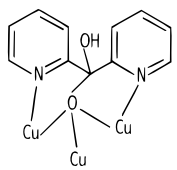

IX

chelating rings with two different metals (these rings share a common C−O edge) and an alkoxide-type bond to a third Cu^{II}

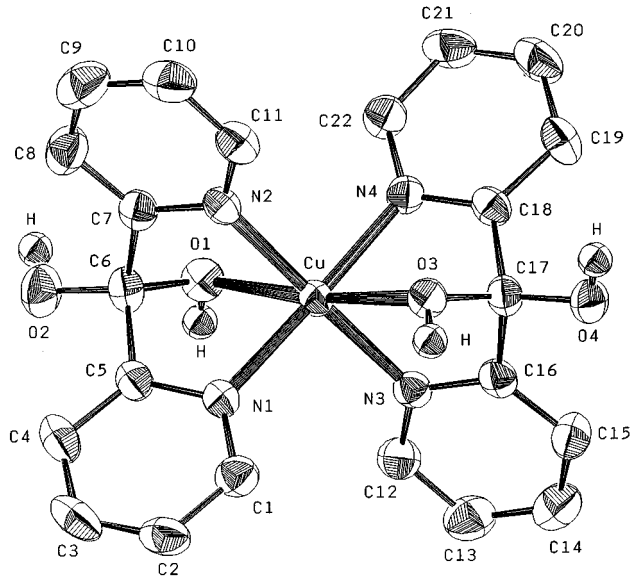

Figure 2. ORTEP representation of the cation of complex **2** at the 50% probability level.

atom. This ligation mode is unprecedented in the coordination chemistry of hydrated di-2-pyridyl ketone.[20b−g] Finally, a terminal monodentate $MeCO_2^-$ group is ligated to Cu(2) (Cu(2)−O(113) = 1.913(4) Å). A complex scheme of intramolecular and intermolecular H-bonds stabilizes the crystal structure.

The Cu(1) and Cu(4) centers have similar highly distorted octahedral coordination geometries (Table 2). One octahedral face is occupied by three bridging, alkoxide-type oxygen atoms, and the other contains three nitrogen atoms from three different ligands. For Cu(3), also six-coordinate, the weak axial interactions (Cu(3)−O(21) = 2.480(3) Å, Cu(3)−O(112′) = 2.711(4) Å) indicate strong Jahn−Teller distortion. The Cu(2) atom lacks the sixth ligand, however, displaying a distorted square pyramidal geometry. Analysis of the shape-determining angles using the approach of Addison *et al.*[25] yields a value for the trigonality index, τ, of 0.27 for Cu(2) (τ = 0 and 1 for perfect sp and tbp geometries, respectively). Thus, the geometry about Cu(2) is significantly distorted. As expected, the axial Cu(2)−O(1) (2.357(3) Å) bond is the longest.

The Cu−O (alkoxide-type) distances are of two types: The axial bond is elongated to an average distance of 2.510 Å compared to the average equatorial distances of 1.986 Å. The Cu···Cu vectors reflect the alternating Cu−O bond lengths in four cube faces (Cu(2)O(31)Cu(4)O(1), Cu(1)O(11)Cu(3)O(21), Cu(1)O(1)Cu(2)O(11), Cu(3)O(21)Cu(4)O(31)). The four diagonals of these cube faces (3.304(1)−3.527(1) Å) are an average of 0.40 Å longer than the two other face diagonal vectors (Cu(1)···Cu(4) = 3.004(1) Å, Cu(2)···Cu(3) = 3.038(1) Å). The Cu(3)···Cu(3′) distance which "bridges" the cubanes is 4.913(1) Å. It is interesting to note that the intraligand pyridyl ring dihedral angles are 76.4, 72.8, 73.9, and 84.8° as compared to 180° for a planar ligand.

The arrangement of four metal ions and four triply-bridging ligands at alternating vertices of a cube is a well-precedented unit in inorganic chemistry.[26] Restricting further discussion to alkoxo-bridged Cu^{II} cubanes, the $[Cu_4(\mu_4\text{-}OR)_4]^{4+}$ core has been structurally characterized in several complexes.[27] There are two distinct types of cubane structures for this class of molecules. According to the Mergehenn and Haase classification,[27g] in type I complexes the four longest Cu−O bonds are parallel while in type II complexes two of the longest Cu−O bonds are perpendicular to the other two longest Cu−O bonds. Type I can be considered as built from two dimers held together by out-of-plane Cu−O bonds, while type II can be considered as derived from an eight-membered Cu_4O_4 ring folded in a boatlike conformation. In the dimer−dimer cubane compounds, Cu···Cu distances within and between dimers are in the ranges 2.90−3.18 and 3.20−3.53 Å, respectively.[27a] Besides these extreme types, there are intermediate types where Cu···Cu separations tend to become equal.[27f,g] Each Cu_4O_4 core of **1** clearly belongs to the type I complexes, with the four, nearly parallel longest bonds in the Cu(1)−Cu(4) cubane being Cu(1)−O(11), Cu(2)−O(1), Cu(3)−O(21), and Cu(4)−O(31) (Figure 1).

Complex **1** joins a very small family of discrete Cu^{II} aggregates of nuclearity eight;[18] as far as we can ascertain, the found topological arrangement of eight metal ions is unique for copper(II).

The structure of **2** consists of the mononuclear $[Cu(dpk{\cdot}H_2O)_2]^{2+}$ cation, one $MeCO_2^-$ anion, one disordered ClO_4^- anion, and two H_2O solvate molecules; the latter three will not be further discussed. The pyridyl nitrogens can be viewed as strongly coordinating to the metal (Cu−N = 2.013(4)−2.022(4) Å), while one of the hydroxyl oxygens on each ligand forms a weak bond to Cu^{II} (Cu−O(1) = 2.417(4) Å, Cu−O(3) = 2.352(3) Å) in the axial direction. Thus, the $dpk{\cdot}H_2O$ molecules adopt the coordination mode **III**. The six-membered ring, Cu−N(1)−C(5)−C(6)−C(7)−N(2), is in a boat conformation, and the mean plane passing through N(1), C(5), C(7), and N(2) leaves the Cu and C(6) atoms −1.009 and −0.775 Å, respectively, out of the plane on the same side. Similarly, the Cu−N(3)−C(16)−C(17)−C(18)−N(4) ring adopts a boat conformation with the Cu and C(17) atoms lying 1.033 and 0.763 Å, respectively, out of the mean plane passing through the other four atoms on the same side. The angles formed between the Cu−O(1) and Cu−O(3) vectors and the normal to the mean equatorial N(1)N(2)N(3)N(4) plane are 22.1 and 19.7°, respectively. The two pyridyl rings of each $dpk{\cdot}H_2O$ ligand are planar and make dihedral angles of 73.7 (N(1)C(1)C(2)C(3)C(4)C(5)/N(2)C(7)C(8)C(9)C(10)C(11)) and 66.8° (N(3)C(12)C(13)C(14)C(15)C(16)/N(4)C(18)C(19)C(20)C(21)C(22)). There is also a complex hydrogen-bonding network, linking H_2O molecules, ClO_4^- and $MeCO_2^-$ counterions, and hydroxyl groups (Table 3).

The structure of the cation of **2**, as detailed in the discussion above and in Table 3, shows remarkable similarity to those[20d] of the cations of $[Cu(dpk{\cdot}H_2O)_2]Cl_2{\cdot}4H_2O$ and $[Cu(dpk{\cdot}H_2O)_2](NO_3)_2{\cdot}2H_2O$. In the latter two structures, however, the Cu^{II} atom sits upon a crystallographic inversion center.

IR and UV/Vis Spectroscopy. In the IR spectra, complex **1** exhibits medium- to strong-intensity bands at 3385 and ∼3300 cm^{-1}, assignable to $\nu(OH)_{dpk{\cdot}OH^-}$ and $\nu(OH)_{H_2O}$, respectively.[28] The broadness and relatively low frequency of these bands are

(25) Addison, A. W.; Rao, T. N.; Reedijk, J.; Rijn, J.; Verschoor, G. C. *J. Chem. Soc., Dalton Trans*. **1984**, 1349.

(26) (a) Demadis, K. D.; Coucouvanis, D. *Inorg. Chem*. **1995**, *34*, 436. (b) Holm, R. H.; Ciurli, S.; Weigel, J. A. *Prog. Inorg. Chem*. **1990**, *38*, 1.

(27) Some representative papers: (a) Wang, S.; Zheng, J.-C.; Hall, J. R.; Thompson, L. K. *Polyhedron* **1994**, *13*, 1039. (b) Fallon, G. D.; Moubaraki, B.; Murray, K. S.; Van den Bergen, A. M.; West, B. O. *Polyhedron* **1993**, *12*, 1989. (c) Schwabe, L.; Haase, W. *J. Chem. Soc., Dalton Trans*. **1985**, 1909. (d) Astheimer, H.; Nepveu, F.; Walz, L.; Haase, W. *J. Chem. Soc., Dalton Trans*. **1985**, 315. (e) Walz, L.; Paulus, H.; Haase, W.; Langhof, H.; Nepveu, F. *J. Chem. Soc., Dalton Trans*. **1983**, 657. (f) Merz, L.; Haase, W. *J. Chem. Soc., Dalton Trans*. **1978**, 1594. (g) Mergehenn, R.; Haase, W. *Acta Crystallogr., Sect. B* **1977**, *33*, 1877. (h) Estes, E. D.; Hodgson, D. J. *Inorg. Chem*. **1975**, *14*, 334.

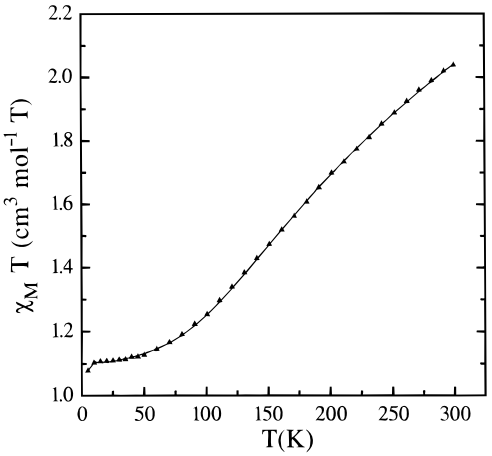

Figure 3. Plot of $\chi_M T/Cu^{II}_4$ vs T for a polycrystalline sample of complex **1**. The solid line results from a least-squares fit of the data to the theoretical model; see Table 7 and the text for fitting parameters.

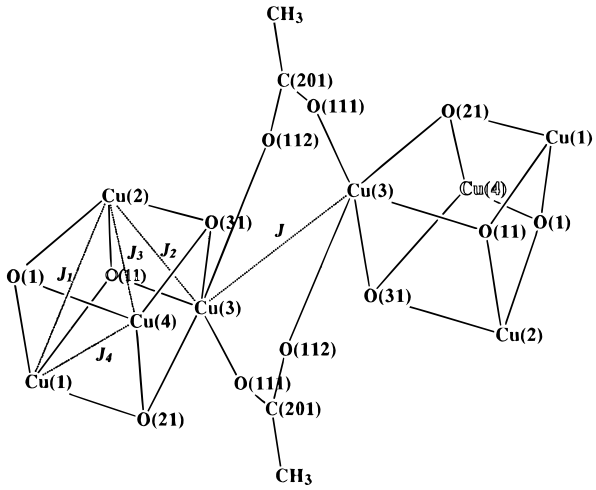

Figure 4. Doubly acetato-bridged dicubane core of complex **1** showing the pairwise magnetic exchange interactions in one of the cubane moieties. To avoid congestion, the Cu(1)···Cu(3) (J_3) and Cu(3)···Cu(4) (J_1) exchange parameters are omitted.

both indicative of strong hydrogen bonding. Complex **2** exhibits relatively broad stretching bands of medium intensity at 3554, 3420, and ~3200 cm^{-1}, due to free O−H of dpk·H_2O, coordinated O−H of dpk·H_2O, and O−H of solvate H_2O, respectively.[28] The spectra of both complexes do not exhibit bands in the region expected for ν(C═O) absorption (1684 cm^{-1} for free dpk), with the nearest IR absorptions at 1602 (**1**) and 1606 (**2**) cm^{-1}, assigned as a pyridine stretching mode raised from 1582 cm^{-1} on coordination, as observed earlier[20e] on complex formation involving hydration of dpk; the strong and rather broad band at 1602 cm^{-1} in **1** also involves ν_{as}(COO) character,[28] as no other strong band is observed in the 1600−1500 cm^{-1} region. The ν_{as}(COO) band of **2** is at 1558 cm^{-1}. The ν_s(COO) modes are difficult to assign, due to the presence of pyridine stretching bands at *ca.* 1450 cm^{-1}. The IR spectra of both complexes exhibit strong bands near 1100 and 625 cm^{-1} due to the $\nu_3(F_2)$ and $\nu_4(F_2)$ modes of the uncoordinated ClO_4^-, respectively.[28] The broad character and splitting of the band at ~1100 cm^{-1} indicate the involvement of the ClO_4^- ion in hydrogen bonding.

The d−d wavelength (725 nm) in the solid-state electronic spectrum of **1** is fairly typical of a square-pyramidal or/and tetragonally-distorted six-coordinate geometry.[29] This complex also possesses a band at 370 nm assigned to O^--to-Cu^{II} or/and $MeCO_2^-$-to-Cu^{II} LMCT transition.[29,30] This spectrum is similar to the solution spectrum in $MeNO_2$, probably indicating that the solid-state structure persists in solution. The d−d spectrum of **2** consists of a featureless band at 595 nm; this wavelength is typical of a distorted *trans*-$Cu^{II}N_4O_2$ chromophore.[29] The complex also exhibits an absorption at 330 nm assignable to an $^-$OH-to-Cu^{II} LMCT transition.[29]

Magnetic Properties of 1. The temperature dependence of the magnetic susceptibility for this compound has already been reported.[22] For completeness, the $\chi_M T$ vs T curve, indicating the presence of antiferromagnetic exchange interaction between the Cu^{II} atoms, where χ_M is the molar paramagnetic susceptibility per cubane moiety, is recalled in Figure 3.

The magnetic behavior of the compound is considered as that of a simple cubane with a molecular field to account for the intercubane magnetic interactions through the two intervening acetato bridges.[31] The reduced Hamiltonian,[32,33] according to Figure 4, is

$$H = -2J_1(S_1 \cdot S_2 + S_3 \cdot S_4) - 2J_2(S_2 \cdot S_3) - 2J_3(S_1 \cdot S_3 + S_4 \cdot S_2) - 2J_4(S_1 \cdot S_4) \quad (4)$$

where all symbols have their usual meaning. The above formula assumes the existence of a 2-fold axis in each cubane entity, while in reality it is only a pseudo-2-fold axis. This assumption was made in order to avoid dealing with a 6-J model. The solution of the corresponding energy matrix yields one quintet level, three triplet levels, and two singlet levels. The expressions for these energy levels are given in ref 31b.

Various models have been used to fit the experimental $\chi_M T$.[22] Moreover we used 2-J and 3-J models in an attempt to confirm the correctness of our 4-J model. The final expression of the calculated molar susceptibility, χ_M, is given in eq 1 of ref 22. The parameter sets[34] derived by using these latter models are given in Table 4. The very low negative J value accounts well for the intercubane interactions inside each dicubane moiety evidenced by the slight decrease of the $\chi_M T$ values below ~8 K.

An inspection of Table 4 clearly shows that, as expected, the fitting becomes better upon increasing the number of parameters. Moreover, it is also clear that in the case of 2-J model ($J_1 = J_3 = 0$), in which a model of two unequal dimers is considered with no interaction between them, we get one high

(28) Nakamoto, K. *Infrared and Raman Spectra of Inorganic and Coordination Compounds*, 4th ed.; Wiley: New York, 1986; pp 227−233, 251, 253.
(29) Lever, A. B. P. *Inorganic Electronic Spectroscopy*, 2nd ed.; Elsevier: Amsterdam, 1984; pp 356, 553−572, 636−638.
(30) Karlin, K. D.; Faroog, A.; Hayes, J. C.; Cohen, B.; Rowe, T. M.; Sinn, E.; Zubieta, J. *Inorg. Chem*. **1987**, *26*, 1271.
(31) (a) Colacio, E.; Costes, J. P.; Kivekäs, R.; Laurent, J.-P.; Ruiz, J. *Inorg. Chem*. **1990**, *29*, 4240. (b) Chiari, B.; Piovesana, O.; Tarantelli, T.; Zanazzi, P. F. *Inorg. Chem*. **1993**, *32*, 4834.
(32) (a) Ginsberg, A. P. *Inorg. Chim. Acta Rev*. **1971**, *5*, 45. (b) Martin, R. L. In *New Pathways in Inorganic Chemistry*; Ebsworth, E. A. V., Maddock, A. G., Sharpe, A. G., Eds.; Cambridge University Press: Cambridge, U.K., 1969; Chapter 9. (c) Sinn, E. *Coord. Chem. Rev*. **1970**, *5*, 313.
(33) Hall, J. W.; Estes, W. E.; Estes, E. D.; Scaringe, R. P.; Hatfield, W. E. *Inorg. Chem*. **1977**, *16*, 1572.
(34) (a) The fitting procedure is described in ref 22. (b) The statistical test of the *R*-factor ratio was used to examine the significance in the improvement of the *R*-factor as we increase the J parameters from 2 to 4. According to this test the improvement in the model from 2-J to 3-J and from 3-J to 4-J is significant at the 0.04 and 0.17 levels. While the latter level is not particularly significant, we include this model because we feel it contains information which is averaged out in the 3-J model (see text).
(35) Bencini, A.; Gatteschi, D. *EPR of Exchange-Coupled Systems*; Springer-Verlag: Heidelberg, Germany, 1990.

Table 4. Sets of Magnetic Parameters[34]

	magnetic model		
param	4-*J*	3-*J*	2-*J*
J_1, cm^{-1}	6(1)	−8(1)	
J_2, cm^{-1}	−144(5)	−140(5)	−144(5)
J_3, cm^{-1}	−14(2)		
J_4, cm^{-1}	3(1)	3(1)	3(1)
J, cm^{-1}	−0.5(1)	−0.5(1)	−0.5(1)
g^a	2.29(1)	2.29(1)	2.29(1)
R^b	2.9×10^{-4}	3.0×10^{-4}	3.2×10^{-4}

[a] g was treated as an adjustable parameter.[35] [b] $\sum_n[(\chi_M T)_{exptl} - (\chi_M T)_{calc}]^2$, with $x = 0.007$.[22]

antiferromagnetic intradimer interaction (−144(5) cm^{-1}) and a low ferromagnetic one (3(1) cm^{-1}). This is also the case with the 4-*J* magnetic model. Moreover, in the case of the 3-*J* model, a kind of averaging of the J_1 value happens deriving from the ferromagnetic J_1 value of 6(1) cm^{-1} and the antiferromagnetic J_3 value of −14(2) cm^{-1} of the 4-*J* model. The high g values derived reflect some systematic error in the data. It should be mentioned here that Lippard and co-workers[21] faced an analogous problem concerning the molecular weight for the calculation of the molar magnetic susceptibility in dinuclear Cu^{II} complexes. The conclusion of their treatment was that using a molecular weight without solvent molecules or with various fractions of solvent affects only the g^2 parameter value of the susceptibility equation and not the coupling constant *J*. Unusually high g values have also been reported in other tetranuclear Cu^{II} clusters.[36] The excellent 4-*J* model fit is also shown in Figure 3.

Ferromagnetic and antiferromagnetic interactions within the same molecule are a principal feature of tetranuclear oxygen-bridged Cu^{II} complexes of the cubane type.[27c−f,37] As it will be shown in the next section, the low symmetry of the Cu_4O_4 core of **1** could account well for the great variation of its exchange parameters. As a matter of fact, the variation of the structural parameters (Cu···Cu distances, Cu−O−Cu angles, and CuO_2Cu dihedral angles) within each Cu_4O_4 core of **1** offers the unique opportunity to study in a more thorough way the magneto−structural correlations in these systems.

Figure 5 shows the energy diagram of the spin states resulting from the interpretation of the exchange parameters using the above described models. The most interesting feature is the triplet ground state of **1** derived in all three models. The low-temperature X-band solution (Figure 6) and powdered (Figure 7) EPR spectra of **1** show a broad feature with $g = 4.0$ corresponding to the half-field transition and a sharp feature at *ca*. 3200 G; a peak at very low magnetic field (centered at *ca*. 125 G) also appears at 5 K and attains significant intensity at 50 K (Figure 7). The first and the last features are probably in line with an integer-spin character of the spectra, hence with a triplet ground state for **1** in both $MeNO_2$ solution and the solid state.[38] This is further substantiated by the decrease of the intensity of the powdered spectrum with the increase of the temperature. As a matter of fact, the peak at very low magnetic field values disappears at room temperature. The feature at *ca*. 3200 G corresponds to the $\Delta M_s = \pm 1$ allowed transition ($g = 2.12(1)$, $A_{||} = 105$ G). Furthermore, since the intercubane value for J is −0.5 cm^{-1}, it is likely that the EPR spectra could not be indicative of the resultant intercubane spin levels, since this interaction is in the order of the energy of the measurement (X-band). However, an overall antiferromagnetic interaction results, depending on the relative magnitudes of the antiferromagnetic and ferromagnetic interactions, related to structural features. Moreover, complex **1** constitutes an example of a compound that allows an adequate characterization of its low-lying levels.[15]

Quantum-Chemical Interpretation of the Exchange Coupling. Calculations were carried out with the parametrization and methods already described.[39] In particular, EHMO SCC calculations[40] were performed on the $[Cu_2(NH_3)_4(OMe)_2]^{2+}$ planar model dimer (D_{2h}) in an attempt to determine the H_{ii}'s of the atoms, by using the FORTICON MAC program.[41] The off-diagonal matrix elements were given by the expression of Wolfsberg−Helmholz;[42] a value of 1.75 for the parameter K was still used. The orbital exponents for the atoms were 1.625 for C, 1.95 for N, 2.275 for O, 1.30 for H, and 2.05 and 1.325 for the 4s and 4p ones of Cu, respectively, as well as two-component 3d orbital of Cu with exponents of 5.95 and 2.30 and relative weights of 0.5933 and 0.5744, respectively. All bond lengths ($R_{Cu-N} = 2.0$ Å, $R_{Cu-O} = 1.95$ Å, $R_{C-C} = 1.4$ Å) and the N−Cu−N angle ($R_{Cu-N} = 95°$) of the model planar system (see **X**) studied were fixed as φ was varied while

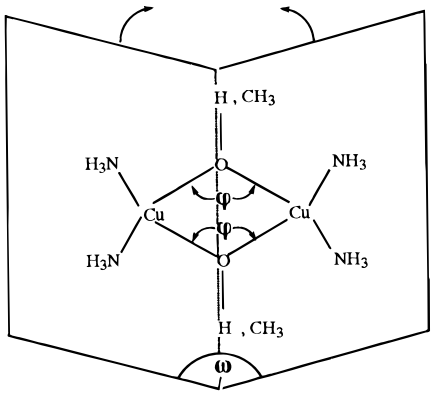

X

maintaining D_{2h} symmetry. However, for the study of the ω, φ dependence of the $\epsilon_A - \epsilon_S = \delta$ difference, all bond lengths were fixed as previously described and H was substituted by the Me group; still, as ω and φ were varied, symmetry was varied from D_{2h} ($\omega = 180°$) to C_{2v} ($\omega \neq 180°$).

As was shown previously, very good agreement between the experimental and calculated susceptibilities down to 5.0 K is obtained by considering a four-parameter (4-*J*) model with a molecular field correction to account for the intercubane interaction in each dicubane entity. The origin of the coexistence of ferromagnetic and antiferromagnetic interactions in **1** can be easily understood by considering first the coordination around each Cu^{II} atom. In particular, Cu(1), Cu(3), and Cu(4) exhibit a 4 + 2 coordination with strongly elongated axial Cu−O and Cu−N bond lengths of *ca*. 2.6 and 2.2 Å,

(36) (a) Tandon, S. A.; Thompson, L. K.; Miller, D. O. *J. Chem. Soc., Chem. Commun.* **1995**, 1907. (b) Rentschler, E.; Gatteschi, D.; Cornia, A.; Fabretti, A. C.; Barra, A.-L.; Shchegolikhina, O. I.; Zhdanov, A. A. *Inorg. Chem.* **1996**, *35*, 4427.
(37) Laurent, J.-P.; Bonnet, J.-J.; Nepveu, F.; Astheimer, H.; Walz, L.; Haaze, W. *J. Chem. Soc., Dalton Trans.* **1982**, 2433.
(38) The decomposition of **1** in solution can be ruled out in accord with the facts that the complex behaves as an 1:4 electrolyte in $MeNO_2$ and its solution- and solid-state electronic spectra are almost identical.
(39) Hay, P. J.; Thibeault, J. C.; Hoffmann, R. *J. Am. Chem. Soc.* **1975**, *97*, 4884 and references therein.
(40) (a) Hoffmann, R. *J. Chem. Phys.* **1963**, *39*, 1397. (b) Hoffmann, R.; Lipscomb, W. N. *J. Chem. Phys.* **1962**, *36*, 3179, 3489; **1962**, *37*, 2872.
(41) Anaxagorou, Th. C.; Katsoulos, G. A.; Sigalas, M. P.; Tsipis, C. A. QCPE QMAC CO20, FORTICON MAC: An interactive version of FORTICON 8. *QCPE Bull.* **1994**, *14*, 5.
(42) Wolfsberg, M.; Helmholz, L. *J. Chem. Phys.* **1952**, *20*, 837.

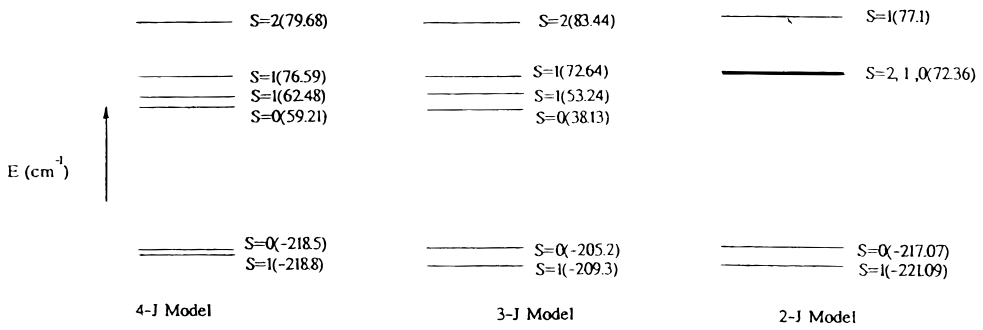

Figure 5. Schematic energy splitting diagram for **1** according to the three models used (see text).

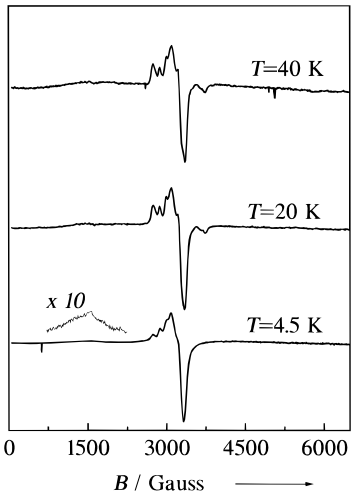

Figure 6. Temperature dependence of the X-band EPR spectrum of a frozen $MeNO_2$ solution of **1**.

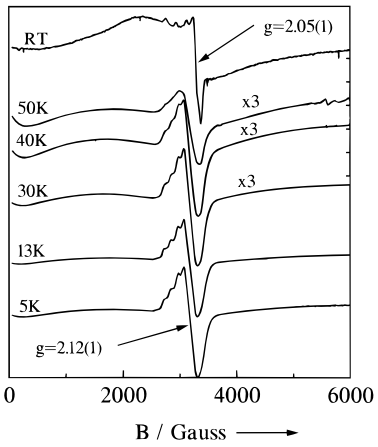

Figure 7. Temperature dependence of the X-band EPR spectrum of a polycrystalline sample of $[Cu_8(dpk{\cdot}OH)_8(O_2CMe)_4](ClO_4)_4{\cdot}9H_2O$ (**1**).

respectively. Hence, the unpaired electron around Cu(1), Cu(3), and Cu(4) is described by a magnetic orbital built from the $d_{x^2-y^2}$ metallic orbital pointing toward its four nearest neighbors, *i.e.* in all three cases toward the O and N atoms of the basal plane. This is also the case, however, with Cu(2), which—despite its 4 + 1 coordination—has a long apical bond (Cu(2)−O(1) = 2.357(3) Å). Thus, the spin densities on the axial O and N donor atoms should be weak. Moreover, each O atom of the cubane skeleton—due to its triply bridging function—belongs, at the same time, to both the magnetic orbitals of the two Cu atoms of each CuO_2Cu entity and to the apical position of a copper of the opposite CuO_2Cu one. It should be stressed here, however, that—due to the low symmetry of **1**—the four calculated *J* values should be compared in pairs since the two antiferromagnetic interactions belong to planar CuO_2Cu entities and the two ferromagnetic ones to roof-shaped[43] alkoxo-bridged Cu^{II} moieties.

The two antiferromagnetic exchange interactions are examined first. The one between Cu(2) and Cu(3) is the strongest antiferromagnetic interaction, whereas that between Cu(1) and Cu(3) is significantly weaker. This is not an unexpected result since, as shown in **XI**, both CuO_2Cu entities under study are

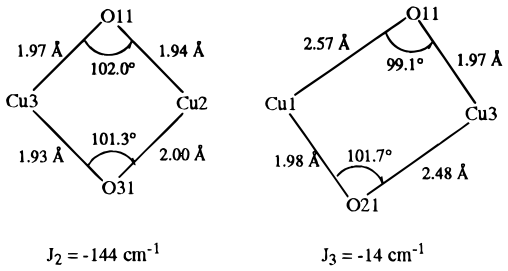

XI

planar and their Cu−O−Cu angles are well above the transition angle (95.7°) established[44] experimentally for the alkoxo-bridged Cu(II) complexes. Consequently, since antiferromagnetic interaction decreases as electron density is removed from bridging atoms,[39] the weaker interaction in the planar $Cu(1)O_2Cu(3)$ entity should be attributed to the reduced electron density on its two O bridges as a result of both its two longer Cu−O bonds and its smaller Cu−O−Cu angle of 99.1°.

However, the Cu(1)···Cu(2) and Cu(1)···Cu(4) interactions are weakly ferromagnetic, their corresponding *J* parameters being +6(1) and +3(1) cm^{-1}, respectively. The planarity observed in both $Cu(2)O_2Cu(3)$ and $Cu(1)O_2Cu(3)$ entities no longer exists in $Cu(1)O_2Cu(2)$ and $Cu(1)O_2Cu(4)$ ones, since their dihedral angles are 158.6 and 159.4°, respectively. Hence, these two latter Cu(II) dinuclear entities should be considered as roof-shaped, alkoxo-bridged dinuclear complexes.[43] As a matter of fact, these two entities have structures similar to that of the dinuclear Cu(II) unit in $Mo_2Cu_2O_4(SALADHP)_2(OMe)_2{\cdot}2MeCN$ (**3**),[43a] their structural differences being mainly in the dihedral CuO_2Cu, ω, and simple Cu−O−Cu, φ, angles. It has been shown[43] that an attenuation in the antiferromagnetic coupling happens upon bending of the OCuO/OCuO dihedral angles in the dinuclear, alkoxo-bridged Cu(II) complexes. Consequently, a ferromagnetic interaction could not be excluded for the exchange interactions in both $Cu(1)O_2Cu(2)$ and $Cu(1)O_2Cu(4)$ entities. Questions that arise now are as follow: (i) Why are the ferromagnetic interactions in **1** weaker than in

(43) (a) Kessissoglou, D. P.; Raptopoulou, C. P.; Bakalbassis, E. G.; Terzis, A.; Mrozinski, J. *Inorg. Chem.* **1992**, *31*, 4339. (b) Charlot, M. F.; Jeannin, S.; Jeannin, Y.; Kahn, O.; Lucrece-Abaul, J.; Martin-Frere, J. *Inorg. Chem.* **1979**, *18*, 1675. (c) Charlot, M. F.; Kahn, O.; Jeannin, S.; Jeannin, Y. *Inorg. Chem.* **1980**, *19*, 1411.
(44) Merz, L.; Haase, W. *J. Chem. Soc., Dalton Trans.* **1980**, 875.

3? (ii) Is an explanation of the ferro- and antiferromagnetism in the alkoxo-bridged roof-shaped Cu(II) complexes, in terms of magneto−structural correlations, possible?

Since the tetrameric cubane complexes can be treated as dimeric subunits, an explanation of the magnetic properties in terms of magneto−structural correlations is possible. In addition to $Cu(1)O_2Cu(2)$ and $Cu(1)O_2Cu(4)$ entities of **1**, structural and magnetic details for the closely related compound **3** are available.[43a]

In our case, the three major structural factors governing the antiferromagnetic interaction are (i) the Cu−O−Cu angle, φ, (ii) the dihedral CuO_2Cu angle, ω, and (iii) the Cu−O bond length. Similar relatioships between J and ω and J and φ had already been established and are inadequate to answer our questions. A three-parameter relation should be established, and as such the ω and φ angles dependence of δ, where δ denotes the energy difference between the symmetric and antisymmetric MOs of the O bridging ligand (symmetry-adapted to interact with the degenerate singly-occupied in- and out-of-phase combinations of the Cu d orbitals), for a constant Cu−O bond distance is examined next.

A 3D drawing of the ω,φ dependence of δ is shown in Figure 8a; a contour plot of the same dependence is provided in Figure 8b. It is clear from Figure 8 that there is a valley, the well of which—corresponding to the crossover point ($\delta = 0$)—starts from the ω and φ pair values of 180 and 81°, respectively, and proceeds through an arc direction to the end, where $\omega = 117.5°$ and $\varphi = 110°$. The upper right part of the contour map strongly exhibits the antiferromagnetic character, whereas the lower part sharply exhibits its ferromagnetic behavior.

The most crucial point emerging from Figure 8a,b is that the crossover point corresponds to a different dihedral angle, ω, for a given φ value. As a matter of fact, not all φ values exhibit the same crossover point value, since ω approaches 180° as φ bends from 110 to 81°. This, in turn, means that, for an ω value greater than 117.5°, ferromagnetic interaction should be more predominant as φ value approaches its lower limit of 81° and/or for the same φ angle ferromagnetic interaction should be less predominant as ω approaches its upper limit of 180°. It is worth noting, however, that the slope of the antiferromagnetic region on the contour plot becomes sharper upon bending of the φ angle from 81 to 110°.

Moreover, Table 5 gives the experimental magnetic and structural data for some structurally characterized cubanes,[27d,e,33,37,43a,44] involving CuO_2Cu moiety configurations with ω values other than 180°. In particular, in Table 5 the exchange parameter, J, of each CuO_2Cu moiety configuration, along with its ω and φ angle values as well as the four Cu−O bond lengths, are listed; additionally, the difference between the two φ angles, denoted as $\Delta\varphi$, for each CuO_2Cu moiety configuration, the Cu−O mean values of the four different corresponding bonds in pairs of the most closely values, denoted as $Cu-O_{mean}$, of each CuO_2Cu, and the mean value of the two φ values of each CuO_2Cu moiety (and/or the smaller of the two if $\Delta\varphi \geq 3.3$), denoted as φ_{mean}, are also presented. First, the CuO_2Cu moieties exhibiting antiferromagnetic interaction are given, in descending order of their exchange parameters (numbering from −1 to −16), then the moiety configuration with J value equal to zero (corresponding symbol, *), and finally those with ferromagnetic interaction also in descending order of their exchange parameters (numbering from 1 to 9) are presented.

Since all CuO_2Cu moieties considered have ω values in the range between 150 and 175°, we have magnified, for clarity, the upper part of Figure 8b. First, in this new Figure 9 the pair

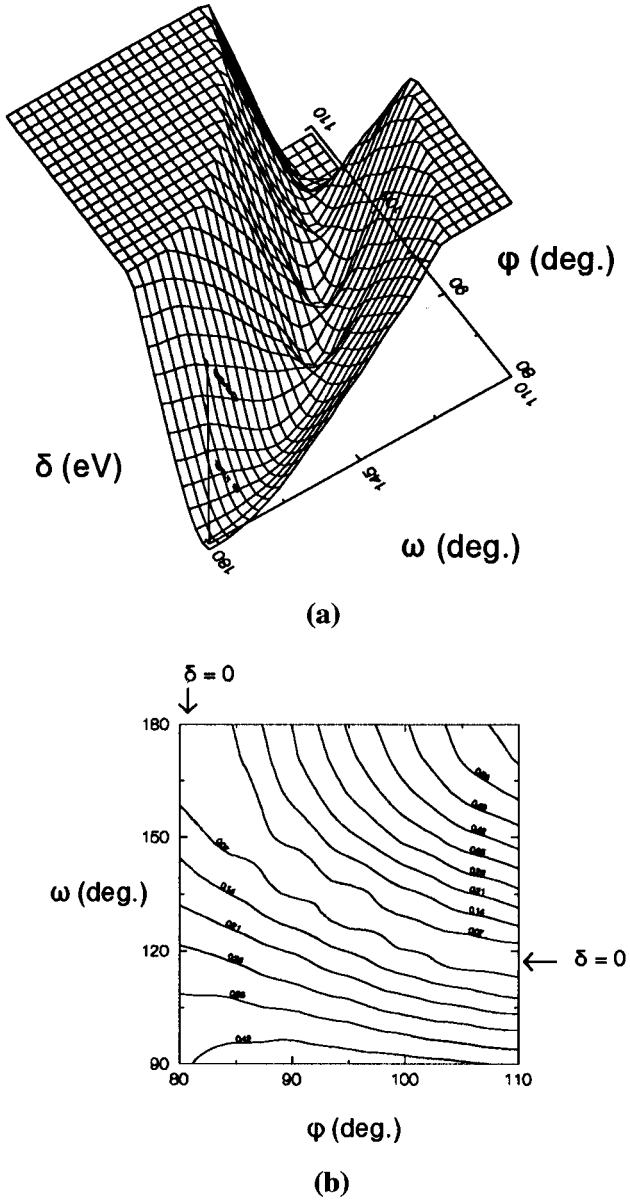

Figure 8. 3D-plot of the ω,φ dependence of δ (a) and contour plot of the same dependence (b). Contour values used range from 0.07 to 0.60 eV.

of the ferromagnetic 1 and 9 CuO_2Cu moieties, having four almost equal Cu−O bond lengths, are shown, according to their φ_{mean},ω pair of values. These two moieties are among the few ones of Table 5 for which a J value can be unambiguously assigned. It is clear from Figure 9 that both 1 and 9 are arranged close to the lower δ values of the well. However, due to its both φ and ω lower values, the former both exhibits stronger ferromagnetism than the latter and lies closer to the well. This, in turn, further verifies the significance of these two structural parameters in the enhancement of the ferromagnetic interaction and makes it our favorite parameter set choice for a magneto−structural criterion. In a subsequent stage, all of the other CuO_2-Cu moiety configurations given in Table 5—despite the possible ambiguity in the assignment of a J value to them—are also shown, according to their φ_{mean},ω pair of values. In the case, however, where $\Delta\varphi$ is greater or equal to 3.3, the smaller φ value of each CuO_2Cu entity configuration was considered in this latter pair of values instead of φ_{mean}.

The complete Figure 9 clearly demonstrates that (i) the majority of ferromagnetic moieties are arranged along the direction of the well and close to its lower δ values, (ii) the

Table 5. Magnetic and Structural Data[a] for CuO_2Cu Moieties Belonging to Structurally Characterized Cubane Complexes

numbering	J, cm^{-1}	ω, deg	φ_{mean}, deg	$\Delta\varphi$, deg	φ, deg	Cu−O_{mean}, Å	Cu−O, Å	ref
−1	−84.1	165.0	98.4	1.3	(99.0; 97.7)	1.91; 2.12	(1.90, 1.92, 2.11, 2.13)	44
−2	−72.0	164.9	98.1	1.0	(98.6; 97.6)	1.92; 2.09	(1.92, 1.93, 2.08, 2.10)	44
−3	−65.1	154.5	97.5	0.6	(97.8; 97.2)	1.94; 1.97	(1.93, 1.95, 1.97, 1.97)	44
−4	−60.0	162.7	97.6	0.0	(97.6; 97.6)	1.94; 1.97	(1.94, 1.94, 1.97, 1.97)	33
−5	−53.0	168.4	99.5	0.0	(99.5; 99.5)	1.91; 2.24	(1.91, 1.91, 2.24, 2.24)	44
−6	−36.2	172.6	99.6	3.8	(99.6; 103.4)	1.96; 2.47	(1.95, 1.97, 2.42, 2.52)	33
−7	−30.0	168.2	98.9	0.0	(98.9; 98.9)	1.93; 2.21	(1.93, 1.93, 2.21, 2.21)	44
−8	−28.1	168.0	98.0	0.8	(97.6; 98.4)	1.93; 2.12	(1.91, 1.94, 2.09, 2.14)	44
−9	−27.0	166.3	97.4	0.4	(97.2; 97.6)	1.92; 2.11	(1.92, 1.93, 2.11, 2.11)	44
−10	−14.9	155.4	95.7	0.0	(95.7; 95.7)	1.95; 1.99	(1.95, 1.95, 1.99, 1.99)	33
−11	−14.8	176.3	93.4	10.9	(93.4; 104.3)	2.01; 2.33; 2.69	(2.00, 2.03, 2.33, 2.69)	27d
−12	−9.3	175.0	97.3	9.2	(97.3; 106.5)	2.00; 2.39; 2.57	(1.95, 2.06, 2.39, 2.57)	27e
−13	−7.1	175.2	104.4	0.0	(104.4; 104.4)	2.00; 2.48	(2.00, 2.00, 2.48, 2.48)	27e
−14	−0.9	161.4	95.2	0.4	(95.0; 95.4)	1.94; 2.00	(1.94, 1.94, 2.00, 2.01)	44
−15	−0.6	157.6	96.1	0.8	(95.7; 96.5)	1.93; 1.98	(1.91, 1.95, 1.97, 1.99)	44
−16	−0.3	157.0	95.8	2.0	(96.8; 94.8)	1.94; 1.97	(1.94, 1.94, 1.95, 1.99)	44
*	0	161.2	93.9	0.0	(93.9; 93.9)	1.98; 2.73	(1.98, 1.98, 2.73, 2.73)	37
1	30.0	150.8	94.9	0.0	(94.9; 94.9)	2.00; 2.00	(1.99, 2.00, 2.00, 2.00)	43a
2	28.5	166.7	89.3	14.9	(89.3; 104.2)	1.97; 2.48	(1.96, 1.96, 2.00, 2.48)	27d
3	24.9	159.5	88.7	12.1	(88.7; 100.8)	1.96; 2.33	(1.95, 1.97, 1.98, 2.33)	27e
4	21.0	170.3	96.7	5.3	(96.7; 102.0)	1.99; 2.27	(1.90, 2.09, 2.26, 2.28)	44
5	17.1	173.9	86.6	25.8	(86.6; 112.4)	1.95; 2.73	(1.95, 1.95, 2.73, 2.73)	37
6	15.0	169.1	96.0	5.0	(96.0; 101.0)	1.97; 2.24; 2.72	(1.92, 2.11, 2.24, 2.72)	44
7	8.0	166.3	93.2	9.7	(93.2; 102.9)	1.93; 2.15; 2.24	(1.93, 2.15, 2.15, 2.24)	44
8	6.0	158.6	93.4	3.3	(93.4; 96.7)	2.00; 2.36; 2.56	(1.94, 2.06, 2.36, 2.56)	this work
9	3.0	159.4	96.5	1.0	(96.0; 97.0)	1.98; 2.04	(1.98, 1.98, 2.03, 2.06)	this work

[a] See text for definitions of the various parameters.

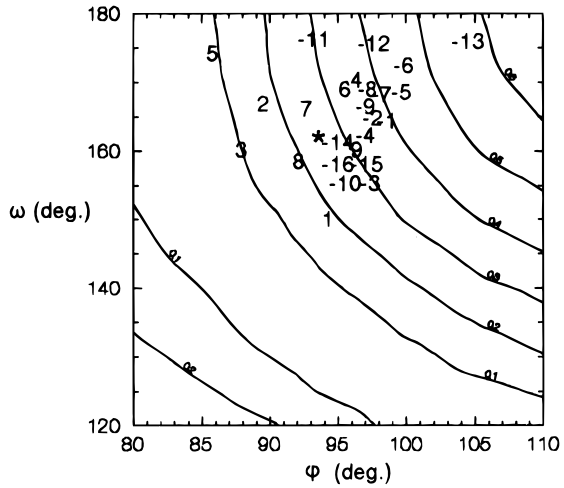

Figure 9. Magnification of the upper part of Figure 8b, on which all different CuO_2Cu moiety configurations, given in Table 5, are also shown.

ones with the antiferromagnetic interaction are spread to the right of the previous moieties, corresponding to areas of the well with medium δ values, and (iii) the moiety with $J = 0$ value is at the borderline between the two classes of moieties. According to Figure 9, one should expect that *ferromagnetic interactions do occur close to the well of the figure, while antiferromagnetic ones do occur at areas on the same hill sides exhibiting higher* δ *values*. It is worthwhile mentioning here that the criterion just derived holds for roof-shaped, alkoxo-bridged CuO_2Cu moiety configurations, involving both four equal Cu−O bonds and two equal φ angles. However, Figure 9 in conjuction with numbers in Table 5 also shows that two or more CuO_2Cu moiety configurations should exhibit J parameters of the same order of magnitude accounting for the fact that both their Cu−O bonds and φ angles are almost equal too. This is actually the case for the −1, −2 and −3, −4 and −7, −8, −9, and −14, −15, −16 pairs/triads of CuO_2Cu moieties, which exhibit in pairs/triads J parameters of the same order, since they involve four almost equal Cu−O bonds and two almost equal φ angles as well as almost equal ω dihedral angles. Finally, as far as the rest CuO_2Cu moieties appearing in Table 5 are concerned, they exhibit J parameters depending mostly on their low symmetry, *i.e.* on their long and unequal Cu−O bonds. This could account well for (i) the fact that some of the ferromagnetic moiety configurations, *e.g.* the 4, 6, and 9 ones, appear to lie among the antiferromagnetic ones and (ii) the abnormal distribution in the corresponding region of some of the antiferromagnetic ones, *e.g.* −11, −12, and −13.

Finally, the *syn, anti* configuration of the $MeCO_2^-$ groups intervening between the cubane moieties together with the long Cu(3)−O(112′) distance could account well for the calculated very weak intercubane antiferromagnetic interaction.

Concluding Comments. We have reported the preparation of the remarkable octanuclear Cu^{II} cluster $[Cu_8(dpk{\cdot}OH)_8(O_2CMe)_4](ClO_4)_4{\cdot}9H_2O$ (**1**), and described its structure and magnetic properties. This complex is interesting from several viewpoints, for it has a novel structure in the solid state and it is one of the rare examples of a magnetically studied Cu^{II}_8 cluster. The cluster constitutes an example of a compound that allows an adequate characterization of its low-lying energy levels. Finally, a new criterion has been established, holding for the magneto−structural correlations in symmetrical roof-shaped, alkoxo-bridged $Cu(OR)_2Cu$ moieties. Work in progress reveals the ability of ligands derived from di-2-pyridyl ketone to stabilize polynuclear carboxylate metal assemblies with an impressive range of nuclearities (M_4−M_{12}) and interesting magnetic properties.

Acknowledgment. This work was supported by the Greek General Secretariat of Research and Technology (Grant 91ED to S.P.P. and PLATON program 1583 to E.B.), Mrs. Athina Athanassiou (V.T.) and the Greek Secretariat of Athletics, OPAP (A.T.).

Supporting Information Available: A table of magnetic *vs* temperature data for **1** (1 page). Two X-ray crystallographic files, in CIF format, are available. Ordering access and information is given on any current masthead page.

IC961137M